Model Study of the Acid−Base Proton-Transfer Reaction of the $ClH\cdots OH_2$ Pair in Low-Polarity Solvents†

Ward H. Thompson‡,§ and James T. Hynes*,§,||

[a]*Department of Chemistry and Biochemistry, University of Colorado, Boulder, Colorado 80309-0215, and Département de Chimie, UMR 8640, Ecole Normale Supérieure, 24, rue Lhomond, 75231 Paris, France*

Received: October 20, 2000

We present a theoretical study of a model of the $ClH\cdots OH_2 \rightleftharpoons Cl^-\cdots HOH_2^+$ acid−base proton-transfer reaction in nonaqueous solvents with low dielectric constants. In this low-polarity environment, both the reactants and products of the proton-transfer reaction are observable. The electronic structure of the acid−base pair is treated via a two-state valence-bond description parametrized using a combination of experimental and ab initio data. The fundamental nature of this proton-transfer reaction is investigated with particular emphasis on the effects of quantization of the proton and hydrogen-bond vibrations. Vibrational wave functions in these coordinates are presented, along with coordinate expectation values and variances, and are placed in the perspective of the proton-transfer process.

I. Introduction

The proton transfer (PT) between the molecular pair HCl and H_2O

$$Cl-H\cdots OH_2 \rightarrow Cl^-\cdots HOH_2^+ \qquad (1)$$

represents an interesting and favorable system in which to examine the effect on the reaction of a quantum-mechanical treatment of the vibrations, the polarity of a surrounding solvent, and the homolytic bond dissociation energy (BDE) of the acid. First, the acid and base are simple: the reaction complex involves only five atoms. Second, the acid ionization of HCl is interesting in its own right and has been studied extensively[1−7] (particularly in water or on ice), which aids in building a reasonable model such as the one we present here. In this paper, the PT reaction 1 in a low-polarity solvent is examined. This yields a case where the reaction is nearly thermoneutral, in contrast to the situation in water where the reaction is very exothermic and almost barrierless.

There is increasing general recognition that nuclear quantum-mechanical effects can be important in PT reactions in solution (see, e.g., refs 1, 2b, and 8−15). Even so, such effects are still often believed to be limited to tunneling of the proton. The importance of quantization of vibrations in the hydrogen-bonded reaction complex in the absence of tunneling is not as well appreciated. In the present work, we simultaneously quantize the vibrations of the proton and hydrogen-bond (H-bond) coordinates in studying the PT reaction. The goal is twofold: to evaluate the importance of a quantum-mechanical description of the H-bond coordinate and to investigate the role of the H-bond coordinate in the PT on the basis of a consistent treatment of the modes.

In a series of papers, Ando and Hynes have examined the ionization of HCl and HF in water using a combination of extensive ab initio calculations and Monte Carlo simulations.[1,16,17] They found that the ionization of HCl in water to produce a contact ion pair occurs essentially without a barrier, whereas for the reaction involving HF, the barrier is ∼2.9 kcal/mol. Their examination of the atomic charges in the reaction complexes (obtained from ab initio calculations) supports the Mulliken picture of PT.[18−21] Specifically, they find that, as the reaction proceeds, a negative charge is transferred from the base (H_2O) to the acid, whereas the charge on the transferring H's charge remains relatively constant with a value of ∼0.3−0.5 (depending on the atomic-charge calculation method). Such a scenario is precisely what is predicted by the Mulliken picture. Accordingly, in developing the valence bond (VB) state potentials within describing the PT in the present study, we adopt a Mulliken perspective.

The outline of the remainder of this paper is as follows. Section II describes the two VB state model used to represent the electronic structure of the hydrogen-bonded $ClH\cdots OH_2$ complex and the dielectric continuum model to account for solvation of the complex in a low-polarity solvent. The details of the quantum treatment of these vibrations and the resulting free-energy surfaces along with the quantal expectation values and variances are given in section III. Finally, concluding remarks are offered in section IV.

II. Outline of the Model

In this Section, we describe a semiempirical two VB state model for the PT reaction in the $ClH\cdots OH_2$ pair that makes use of ab initio calculations on the gas-phase complex. We first discuss the determination of the VB potential-energy surfaces in the gas phase and then outline the incorporation of nonequilibrium solvation effects.

A. Gas-Phase Potentials. We use a semiempirical two VB state model to describe the electronic structure for the PT reaction, with the two VB states being those appropriate for the Mulliken picture of PT.[1,13,14,16−18,20,22,23] Mulliken proposed

† Part of the special issue "William H. Miller Festschrift".

* To whom correspondence should be addressed.

‡ Address as of January 1, 2001: Department of Chemistry, University of Kansas, Lawrence, KS 66045.

§ University of Colorado.

|| Ecole Normale Supérieure.

10.1021/jp003880c CCC: $20.00
Published on Web 01/31/2001

that a PT reaction occurs as a concerted electron−hydrogen atom transfer,[18] that is, that the reaction proceeds by a synchronous transfer of electron density from a lone pair orbital on the base to the antibonding orbital of the acid (A−H bond) and the transfer of a hydrogen atom from the acid to the base. The transfer of electron density to the antibonding orbital weakens the A−H bond just as the A−H bond stretching lowers the antibonding orbital's energy. Thus, the electron and hydrogen atom transfers act in concert to complete the net PT. Therefore, the neutral (N) state (appropriate to the reactants) in our model has the charge character $ClH\cdots OH_2$ and the ionic (I) state (appropriate to the products) has the charge character $[Cl^-\cdots H\cdots OH_2^+$.] These states will be found to have strong electronic coupling between them, such that the transferring species carries a partial-charge intermediate between that of a canonical proton and an H atom. All calculations are carried out assuming a linear Cl−H−O arrangement,[24] with the hydrogens in the water molecule fixed relative to the oxygen. The VB energy surfaces are based on empirical and ab initio data, and the electronic coupling is obtained (vide infra) by requiring that these VB surfaces give the correct adiabatic ground-state surface as determined by ab initio calculations at the MP2/6-31++G** level.[25] Optimized geometries of the $ClH\cdots OH_2$ dimer at this level[26] agree well with previous B3LYP[27] and MP2[28] calculations.

It is important to note at the outset that our model potentials do not accurately represent $ClH\cdots OH_2$ at large Cl−O distances. In particular, the ab initio calculations at this level do not correctly reproduce bond dissociation energies in the system. However, this does not pose a problem, because the model potential and ab initio results are appropriate for the limited range of coordinates relevant to the PT reaction within the complex, the reaction of interest here.

We first consider the neutral VB state. The potential-energy surface for this state is given as a sum of pairwise interaction terms:

$$V_N(r_{HCl}, r_{OH}; R_{ClO}) = V_{HCl}(r_{HCl}) + V_{ClO}(R_{ClO}) + V_{OH}(r_{OH}) \quad (2)$$

where, given the linear Cl−H−O arrangement, R_{ClO} is a redundant coordinate that is fully determined by r_{HCl} and r_{OH}, $R_{ClO} = r_{HCl} + r_{OH}$. Here $V_{HCl}(r_{HCl})$ describes the potential for the H−Cl bond and is given by a Morse function. An extra repulsive potential is added to make the dependence on the coordinate at small r_{HCl} consistent with the ab initio calculations.[29] Thus, the potential is given by

$$V_{HCl}(r_{HCl}) = D_{HCl}[1 - \exp(-\beta_{HCl}(r_{HCl} - r_{HCl}^{e}))]^2 + (\sigma_{HCl}/r_{HCl})^{10} \quad (3)$$

The potential $V_{OH}(r_{OH})$ is the interaction between the transferring H and the water molecule. It includes Coulombic factors due to the water molecule's charge distribution and the assumption that the H in HCl has a finite charge (providing dipole moments for the HCl and H_2O moieties). In addition, a weakly repulsive term is added to represent the potential for small r_{OH}. Thus, we have

$$V_{OH}(r_{OH}) = 4\epsilon_{OH}(\sigma_{OH}/r_{OH})^6 + q_{On}q_{Hn}/r_{OH} + 2q_{Hn}q_{Hwn}/r_{HHw} \quad (4)$$

where the n in the subscripts indicates charges for the neutral form. Further, Hn indicates the H in HCl, Hwn indicates an H in the water molecule, and r_{HHw} indicates the distances between those two atoms (because of symmetry, the distances between the transferring H and each H in the water molecule are always the same). Finally, $V_{ClO}(R_{ClO})$ is the interaction between Cl and the oxygen of the water molecule. It is given by

$$V_{ClO}(R_{ClO}) = A_{ClO}\exp[-B_{ClO}(R_{ClO} - q_{ClO})] + q_{Cln}q_{On}/R_{ClO} + 2q_{Cln}q_{Hwn}/r_{ClHw} \quad (5)$$

where the notation for charges is analogous to that just described. The parameters for the potentials for this VB state are given in Table 1.

TABLE 1: Parameters for the Neutral ($ClH\cdots OH_2$) VB State Potential

parameter	value
Morse Parameters	
D_{HCl} (eV)	4.617
β_{HCl} ($Å^{-1}$)	1.868
r_{HCl}^{e} (Å)	1.2746
Repulsive Potential Parameters	
σ_{HCl} (Å)	0.6318
ϵ_{OH} (eV)	2.940×10^{-4}
σ_{OH} (Å)	0.9525
A_{ClO} (eV)	0.0116
B_{ClO} ($Å^{-1}$)	3.2125
q_{ClO} (Å)	1.6934
Charges	
q(Cln)	−0.10
q(Hn)	+0.10
q(On)	−0.40
q(Hwn)	+0.20

Next we consider the I VB state, for which the form of the potential is analogous to that for the N state. Specifically, it is given by a sum of pairwise interactions:

$$V_I(r_{HCl}, r_{OH}; R_{ClO}) = V_{HCl^-}(r_{HCl}) + V_{Cl-O^+}(R_{ClO}) + V_{O^+H}(r_{OH}) \quad (6)$$

Here the interaction between the transferring H and the chloride ion is

$$V_{HCl^-}(r_{HCl}) = (\sigma_{HCli}/r_{HCl})^{12} + q_{Hi}q_{Cli}/r_{HCl} \quad (7)$$

where now q_{Hi} and q_{Cli} are the charges in the I VB state on the respective species. The interaction between the transferring H and the water molecule is that of hydronium dissociating to give $H^\bullet$ and H_2O^+. The parameters describing this potential are taken from experimental data.[30] The form of the potential is

$$V_{O^+H}(r_{OH}) = D_{hyd}[1 - \exp(-2\beta_{hyd}(r_{OH} - r_{hyd}^{e})]^2 \quad (8)$$

where hyd stands for hydronium. Finally, we have the interaction between the chloride ion and the H_2O^+ species. It is given by

$$V_{Cl-O^+}(R_{ClO}) = 4\epsilon_{ClOi}(\sigma_{ClOi}/R_{ClO})^{12} + q_{Cli}q_{Oi}/R_{ClO} + 2q_{Cli}q_{Hwi}/r_{ClHw} \quad (9)$$

The values used for the parameters appearing in these potentials are given in Table 2.

In the next step, the combination of these VB states and the ab initio calculations of the ground electronic adiabatic surface, $V_{gr}(r_{HCl}, r_{OH}; R_{ClO})$, at the MP2/6-31++G** level can be used to obtain the electronic coupling by the equation

$$V_{coup}(r_{HCl}, r_{OH}; R_{ClO}) = [(V_N - V_{gr})(V_I - V_{gr})]^{1/2} \quad (10)$$

TABLE 2: Parameters for the Ionic ($Cl^-\cdots H\cdots OH_2^+$) VB State Potential

parameter	value
Morse Parameters	
D_{hyd} (eV)	6.2362
β_{hyd} ($Å^{-1}$)	1.7952
r_{hyd}^e (Å)	1.1377
Repulsive Potential Parameters	
σ_{HCli} (Å)	0.7673
ϵ_{ClOi} (eV)	1.4290×10^{-4}
σ_{ClOi} (Å)	3.0898
Charges	
q(Cli)	−1.00
q(Hi)	+0.38
q(Oi)	−0.04
q(Hwi)	+0.33

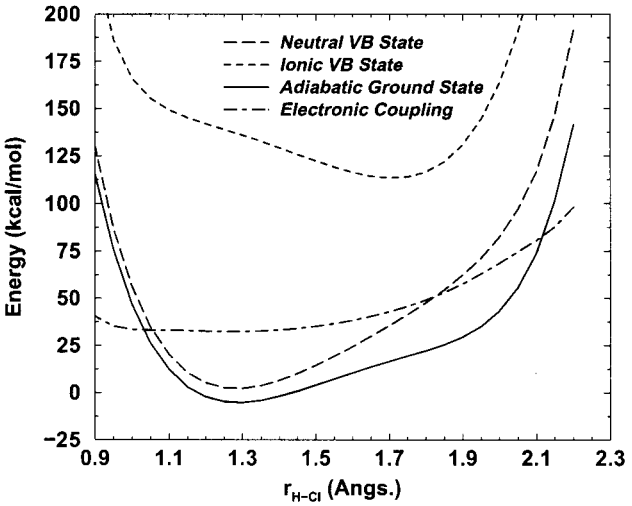

Figure 1. One-dimensional slice through the gas-phase potential surfaces, at $R_{ClO} = 2.9$ Å for the $ClH\cdots OH_2$ system. The semiempirical VB surfaces are shown along with the ab initio ground-state adiabatic potential and the electronic coupling.

The coupling can be obtained in this way for any values of r_{HCl} and r_{OH} of interest for which ab initio calculations are performed. In practice, the ground-state energy, V_{gr}, is calculated on a two-dimensional grid in r_{HCl} and r_{OH}, and a two-dimensional spline interpolation[31] is used to obtain the energy at any set of coordinates within the outer boundaries of the grid. The ab initio calculations were carried out for a grid with spacings of 0.05 Å in both r_{HCl} and r_{OH} for 0.9 Å < r_{HCl} < 3.55 Å and 0.7 Å < r_{OH} < 2.45 Å. As is discussed above, because the ab initio calculations do not have the necessary accuracy for all possible coordinates, the potential is applicable only for a limited region of coordinates. However, this poses no problem for examining the PT within the hydrogen-bonded complex, because the valid range of coordinates is sufficient for describing the reaction to form a contact ion pair.

A one-dimensional slice through the gas-phase potential surfaces is shown in Figure 1. As expected, the N and I VB state surfaces have minima at small ($ClH\cdots OH_2$) and large ($Cl^-\cdots HOH_2^+$) r_{HCl} distances, respectively. In the gas-phase dimer adiabatic potential however, there is no local minimum corresponding to $Cl^-\cdots HOH_2^+$, rather it appears as a flattening of the potential at larger r_{HCl} distances. Finally, the electronic coupling displays an interesting feature in that it increases with the r_{HCl} coordinate (for fixed R_{ClO}), a result differing from other acid−base systems[20] for which the electronic coupling is typically independent of the proton coordinate. The origin of this behavior is discussed in the Appendix.

B. Nonequilibrium Solvation. The gas-phase $ClH\cdots OH_2$ system just described is "solvated" in a dielectric continuum using the fully nonequilibrium Kim−Hynes theory.[32] In this approach, the solvent polarization is given by

$$\mathbf{P}(r) = \mathbf{P}_e(r) + \mathbf{P}_o(r) \tag{11}$$

where $\mathbf{P}_e(r)$ represents the polarization of the solvent electronic degrees of freedom and $\mathbf{P}_o(r)$ represents the (slower) orientational polarization of the solvent associated with translational and rotational degrees of freedom of the solvent molecules. It is assumed that the (fast) electronic polarization is always in equilibrium with the appropriate (vide infra) solute ($ClH\cdots OH_2$) charge distribution, whereas the orientational polarization can take on any (nonequilibrium) value. The interaction of the solute charge distribution with the solvent is considered to occur only through the dipole moment of the solute complex. The diagonal and off-diagonal dipole moments for the PT complex for the different VB states are taken to be $\mu_N = 2.5$ D, $\mu_I = 9.5$ D, and $\mu_{NI} = 1.2$ D. These dipole moment values are taken as those that reproduce reasonably well the free-energy curve for the PT in aqueous solution obtained by Ando and Hynes[1] in combined electronic structure/Monte Carlo simulations. The solvent coordinate, which is a measure of the orientational polarization, is defined in terms of the VB state dipole moments as

$$z \equiv s\mu_I + (1 - s)\mu_N \tag{12}$$

Here, s is a somewhat different solvent coordinate which is defined according to the relation

$$\mathbf{P}_o(r) = \frac{\epsilon_\infty}{4\pi}\left(\frac{1}{\epsilon_\infty} - \frac{1}{\epsilon}\right)[s\,\boldsymbol{E}_I(r) + (1 - s)\,\boldsymbol{E}_N(r)] \tag{13}$$

where $\boldsymbol{E}_I(r)$ is the electric field associated with the I VB state and similarly for $\boldsymbol{E}_N(r)$. The coordinate z can be thought of as specifying an effective dipole moment with which the actual nonequilibrium solvent polarization field would be in equilibrium and thus is, e.g., larger for larger nonequilibrium polarization.[20]

Briefly, in this formulation,[20,32] the free energy of the PT complex in a solvent with optical and static dielectric constants ϵ_∞ and ϵ is given by

$$G_{gr} = c_N{}^2V_N + c_I{}^2V_I - 2c_Nc_I|V_{coup}| + K\left[-z\langle\mu\rangle + \frac{1}{2}z^2\right] - \frac{1}{2}K'\left[\langle\mu^2\rangle - \frac{\rho}{2c_Nc_I + \rho}(\langle\mu^2\rangle - \langle\mu\rangle^2)\right] \tag{14}$$

where the coefficients c_N and c_I are those in the expansion of the ground-state electronic wave function in terms of the VB states:

$$\Psi_g = c_N\psi_N + c_I\psi_I \tag{15}$$

The average dipole moments are $\langle\mu\rangle = c_N{}^2\mu_N + c_I{}^2\mu_I + 2c_Nc_I\mu_{NI}$ and $\langle\mu^2\rangle = c_N{}^2(\mu_N{}^2 + \mu_{NI}{}^2) + c_I{}^2(\mu_I{}^2 + \mu_{NI}{}^2) + 2c_Nc_I\mu_{NI}(\mu_N + \mu_I)$. The constants $K = 2M_s(1/\epsilon_\infty - 1/\epsilon)$ and $K' = 2M_s(1 - 1/\epsilon_\infty)$ can be thought of as force constants for the solvent. The self-energy M_s is taken to be $M_s = 3.74 \times 10^{-3}$ atomic units, which corresponds to, assuming that the solute resides in a spherical cavity of radius 2.7 Å, a reasonable value given the size of the hydrogen-bonded complex. The free-energy surfaces are, in fact, fairly sensitive to this radius; however, similar

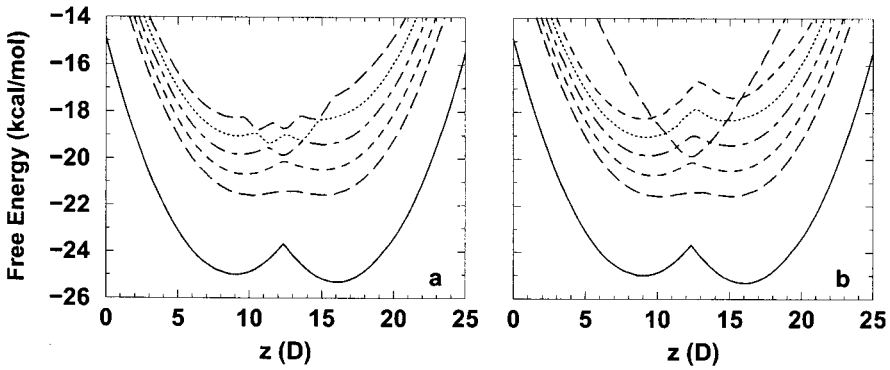

Figure 2. Vibrationally adiabatic (a) and diabatic (b) free-energy surfaces as a function of the solvent coordinate z for ClH···OH_2 in a solvent with $\epsilon_\infty = 2$ and $\epsilon = 13$. Both the bare free-energy surface (solid line) and the first five vibrationally adiabatic surfaces are shown on the left. The bare free-energy surface and schematic representations of the (0, 0−4) and (1, 0) vibrationally diabatic surfaces are shown on the right. (Note that some vibrationally diabatic levels that are lower in energy in the TS region, i.e., the (1, 1) and (1, 2) states, than those plotted here are not shown.)

behavior is observed with different radii but at different static dielectric constants. The factor $\rho \equiv 2|V'_{coup}|\hbar\omega_e$, where V'_{coup} is the solvent-renormalized electronic coupling and ω_e is the average frequency of the solvent electronic polarization (taken to be the electronic absorption frequency of the solvent) and is related to the time scales of motion of the solute and solvent electronic degrees of freedom. In the present work, the solvent electronic frequency is taken as $\omega_e = 0.2$ au, which corresponds to an absorption wavelength of 227.5 nm (chosen as a reasonable value from a survey of several low-polarity solvents).[33]

The coefficients of the VB states in the ground adiabatic electronic state of the solute complex are obtained by solving the nonlinear Schrödinger equation[32] which follows from eq 14, and the reader is directed to ref 32 for the details of the basic procedure. These coefficients are used in eq 14 to obtain the free energy of the complex in its electronic ground state.

III. Results

In this section, we present the results of calculations on the PT reaction 1 using the model described in section II. Specifically, we display and discuss the calculated free-energy surfaces relevant to the reaction and the expectation values and variances of the proton and H-bond (Cl−O) coordinates as a function of solvent coordinate, with an emphasis throughout on issues associated with the quantized proton and H-bond coordinate vibrations.

A. Free-Energy Surfaces. The solvated two degrees-of-freedom electronically adiabatic ground-state free-energy surface is obtained at each value of the solvent coordinate z in the coordinates r_{HCl} and r_{OH} (as described in section II).[34] The H atom and hydrogen bond (Cl−O) motion are quantized simultaneously (i.e., no nuclear adiabatic approximation is invoked between these modes). Several minor approximations are made in calculating the vibrational states of the complex, as are now detailed. First, the water molecule is assumed to move as a single rigid molecule with the center of mass located at the oxygen atom. The kinetic energy operator of this pseudoatom−diatom system is separable in the Jacobi coordinates of the complex, r_{HCl} and R_J, where R_J is the distance from the oxygen atom to the center of mass of the H−Cl diatom. Second, we assume that the center of mass of the diatom is located at the chlorine, so that $R_J = R_{ClO}$, which is an excellent approximation. Then, the vibrational Hamiltonian is

$$\hat{H}_{vib}(z) = -\frac{\hbar^2}{2\mu_{ClO}}\frac{\partial^2}{\partial R_{ClO}{}^2} - \frac{\hbar^2}{2\mu_{HCl}}\frac{\partial^2}{\partial r_{HCl}{}^2} + \hat{G}_{gr}(r_{HCl}, R_{ClO}; z) \quad (16)$$

where μ_{ClO} and μ_{HCl} are the reduced masses for the Cl−H_2O and H−Cl pairs, respectively, and $G_{gr}(r_{HCl}, R_{ClO}; z)$ is obtained from eq 14. The vibrational Schrödinger equation

$$\hat{H}_{vib}(z)\Psi_n(r_{HCl}, R_{ClO}; z) = \epsilon_n(z)\Psi_n(r_{HCl}, R_{ClO}; z) \quad (17)$$

is solved by constructing the Hamiltonian matrix in a sinc-function discrete variable representation basis[35] and obtaining the eigenvalues and eigenvectors through standard "black-box" diagonalization routines. In this way, as many levels as are needed can be obtained.

From these curves, the reaction free energy $\Delta G_{rxn} = G_P - G_R$ and the free-energy barrier $\Delta G^\ddagger = G^\ddagger - G_R$ can be readily obtained from the free energies of the stationary points with respect to z. We will consider primarily the ΔG_{rxn} and $\Delta G^\ddagger$ values associated with the ground adiabatic vibrational state. The surface obtained by minimizing the free energy with respect to r_{HCl} and R_{ClO} will be referred to as the "bare" free-energy surface; naturally, this surface includes no quantization of any of the vibrational modes. In such a decomposition, previously used in refs 2b and 36, the total free energy thus comprises the bare free energy plus the quantum vibrational contribution of the solute pair nuclear modes.

The bare free-energy surface, the first five vibrationally adiabatic surfaces, and a schematic representation of a vibrationally diabatic surface are shown in Figure 2 for the [ClH···OH_2] complex in a solvent with $\epsilon_\infty = 2$ and $\epsilon = 13$. This value of the static dielectric constant, which is close to that of methyl chloride, is chosen because it gives a situation where a reaction can occur, i.e., the free-energy surface has reactant and product minima separated by a barrier (albeit a small one in this case). This figure provides us with a view of the free-energy surface as a function of the reaction coordinate, which can be considered to be the solvent coordinate z. The reactant well occurs at smaller values of z and is apparent as a local minimum in the bare surface and the lowest one or two vibrationally adiabatic surfaces. The product well is identifiable as a local minimum at larger z values, and the transition state (TS) is, naturally, the local maximum lying between the reactants and products. In the surfaces corresponding to greater vibrational excitation, additional structure makes a straightforward identification of the reactants, products, and TS more difficult.

From the free-energy surfaces in Figure 2, we can see that reaction 1 is very slightly endothermic, $\Delta G_{rxn} = 0.007$ kcal/mol, and has only a very small barrier above the endothermicity, $\Delta G^\ddagger = 0.17$ kcal/mol. These values are for the vibrationally adiabatic ground state; for the bare barrier, $\Delta G_{rxn} = -0.32$ kcal/

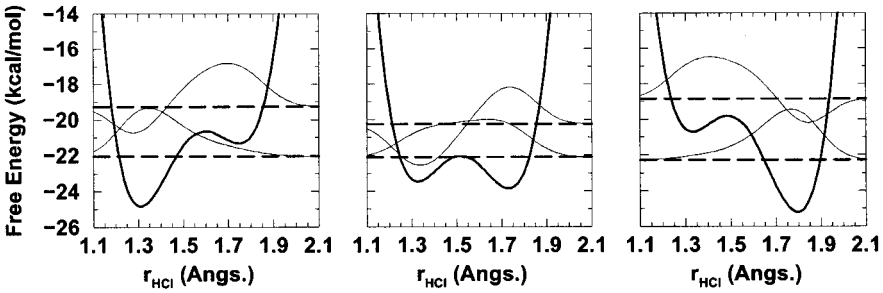

Figure 3. One-dimensional proton potentials, ground and first-excited-state proton vibrational energy levels, and associated vibrational wave functions as a function of r_{HCl} for the $ClH\cdots OH_2$ complex at three values of the solvent coordinate, $z = z_R = 10.1$ D (reactants), $z^{\ddagger} = 12.6$ D (TS), and $z = z_P = 15.1$ D (products), from left to right. These potentials are evaluated at the specified value of fixed z and at fixed R_{ClO} corresponding to the average $\langle R_{ClO} \rangle$ from the full two degrees-of-freedom wave function calculated at that z. The thick solid line is the potential felt by the proton, the energy levels are indicated by the thick dashed lines, and the wave functions are shown as the thin solid lines.

mol and $\Delta G^{\ddagger} = 1.32$ kcal/mol. It is clear that the quantization of the vibrations significantly affects the thermodynamics of the reaction.[2b,36]

A schematic picture of the vibrationally diabatic energy levels of the reaction complex is displayed Figure 2b. The curves were obtained by roughly interpolating across the avoided crossings observed in the vibrationally adiabatic surfaces to connect regions with the same nodal structure in the vibrational wave functions. The vibrational energy curves can be assigned to specific excitations according to the labeling (ν_{Cl-H}, ν_{Cl-O}) by direct examination of the two degrees-of-freedom vibrational wave functions at each value of the solvent coordinate (as is shown in more detail below). It is important to note that these assignments are vibrationally *diabatic* ones. That is, a given vibrationally adiabatic state can have different (ν_{Cl-H}, ν_{Cl-O}) assignments at different values of the solvent coordinate (vide infra). The (0, 0−4) and (1, 0) vibrationally diabatic levels are shown in Figure 2. An important point here is that the vibrational ground state (0, 0) and (especially) first-excited state in the proton vibration (1, 0) have the structure predicted previously by Kim et al.[37] in a study of infrared-induced PT (see also ref 16). This observation, along with the apparent vibrational diabaticity observed here (and discussed below) is encouraging for the prospects for promoting PT by infrared excitation.

The reactant minimum in the vibrationally adiabatic ground state is located at $z = 10.1$ D, whereas the product minimum is found at $z = 15.1$ D. The TS is located at $z = 12.6$ D. To examine the nature of the proton vibrations at the critical points, one-dimensional cuts in the potential in the r_{HCl} coordinate at these three values of the solvent coordinate are shown in Figure 3. Also shown are the two lowest vibrational energy levels of the potential and the corresponding wave functions. These calculations are carried out for fixed R_{ClO}, which has been set equal to the expectation value in the full two degrees-of-freedom wave function at the given value of z. Note that, in its vibrational ground state, the proton is localized on the acid and the base in the reactant and product minima, respectively. It is interesting that the proton is fairly delocalized in the proton first-excited vibrational state in both the reactants and products. However, at the TS, the proton experiences a double-well (but not symmetric) potential and is delocalized in both its ground and first-excited states. The different frequencies of the Cl−H and $H-OH_2^+$ bonds in the reactants and products, respectively, lead to the asymmetry in the double-well potential both in the shape and depth of the wells. The proton zero point energy is just at the top of the barrier in the proton coordinate. The first-excited-state energy level of the H−Cl vibration is ∼1.8 kcal/mol higher in energy than the zero-point energy.

The structure of the vibrational levels of the acid−base complex has a number of notable features. Contour plots of the lowest four vibrationally adiabatic wave functions are shown in Figure 4 as a function of R_{ClO} and r_{HCl} for three values of the solvent coordinate corresponding to the reactants, the TS, and the products in the vibrationally adiabatic ground state (see Figure 2). Also shown are contour plots of the free energy in these coordinates.

It can be seen from the plots of the two degrees-of-freedom free-energy surfaces in Figure 2 that in the reactant and product regions the complex possesses a single local minimum. This localization is also evident in the vibrationally adiabatic vibrational wave functions in Figure 2, which show the wave function localized in the $Cl-H\cdots OH_2$ and $Cl^-\cdots HOH_2^+$ wells when the solvent coordinate is at the reactant and product minima, respectively. The potential felt by the proton is clearly dependent on the R_{ClO} coordinate. In particular, when the solvent coordinate is at its TS value, the potential displays a double-well structure in the proton coordinate, with the shape of the double well strongly modulated by the H-bond coordinate. In this TS region, the ground-state wave function is delocalized between the reactant and product structures. Note that the vibrational zero point energy is above the barrier to PT at this solvent coordinate and the wave function has a single broad peak in the proton coordinate.

The first-excited vibrationally adiabatic free-energy surface has the character of (0, 1) for all values of the solvent coordinate; that is, the vibrational excitation is primarily in the H-bond (R_{ClO}) mode. Note from Figure 2 that in this state the barrier for PT (although still small) is larger than that in the vibrational ground state, i.e., H-bond vibrational excitation slows the PT reaction. This is a general feature previously found by Staib et al.[13] and is easily seen here. The more highly vibrationally excited states exhibit additional features (i.e., beyond that of two local minima separated by a barrier) because of avoided crossings associated with the crossing of the vibrationally diabatic (0, ν_{Cl-O}) and (1, 0) states. The picture is clearer, however, in the representation of the vibrationally diabatic states in Figure 2. There, the increase in the barrier to PT with increasing ν_{Cl-O} is readily observable for up to $\nu_{Cl-O} = 4$. Similarly, the reaction is seen to become more endothermic when the R_{ClO} vibration is excited because of the larger frequency of $H-OH_2^+$ relative to that in H−Cl.

In the second vibrationally adiabatic excited state, the vibrational character is (0, 2) in the reactant and product wells but is (1, 0) at the TS. The energy required to excite the proton vibration $\Delta E_{01} = E_{\nu_{Cl-H}=1} - E_{\nu_{Cl-H}=0}$ is strongly solvent coordinate-dependent, being large in the reactant and product regions and decreasing toward the TS. This is a consequence of the delocalization of the wave function in the r_{HCl} coordinate in the TS region where the $ClH\cdots OH_2$ and $Cl^-\cdots H\cdots OH_2^+$ configurations are close in energy (see Figure 3), as opposed

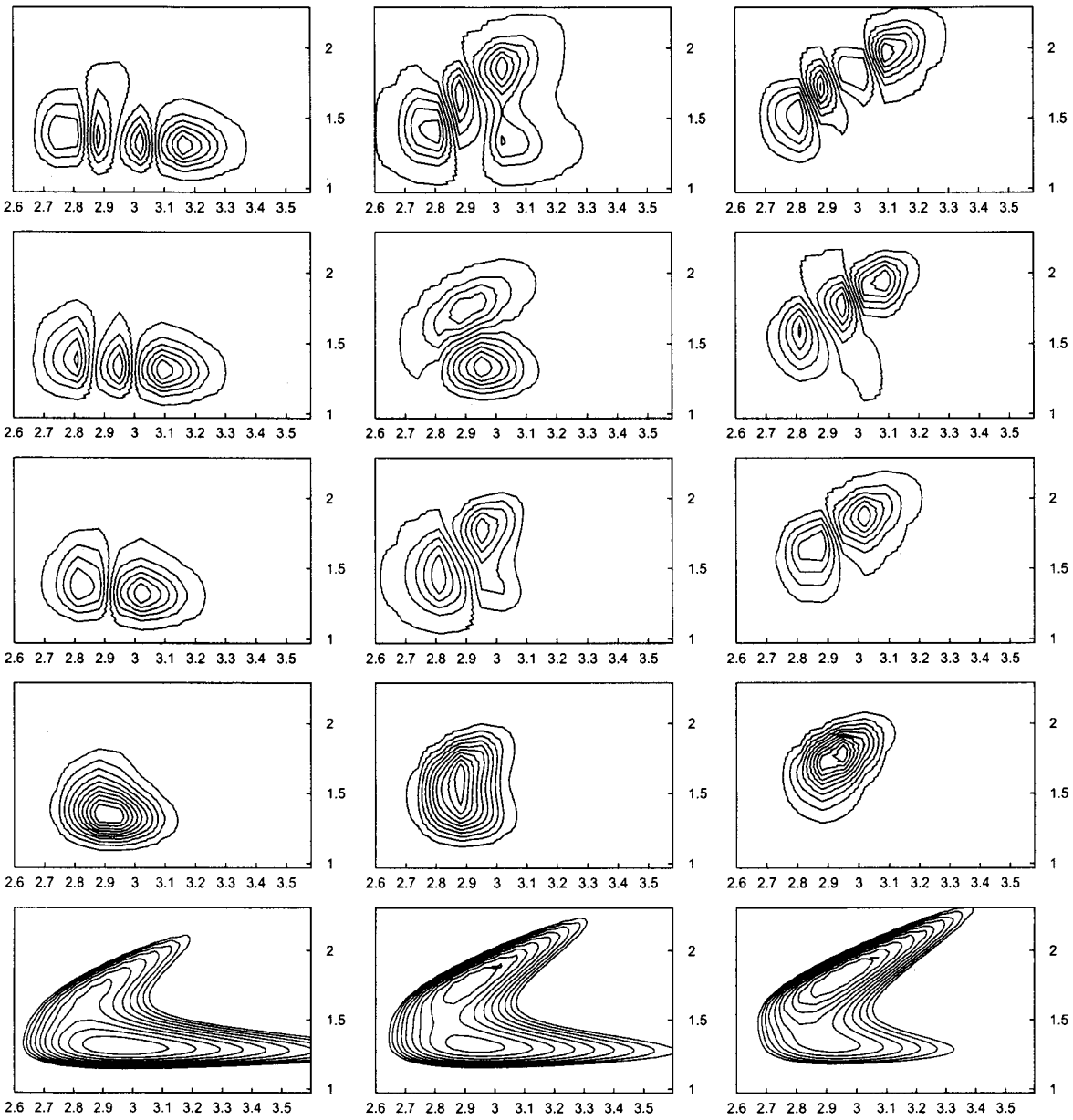

Figure 4. Contour plots of the two degrees-of-freedom free-energy surface (lowest panels) and vibrational wave functions (upper panels) at z = 10.1 D (reactants, shown on the left), z = 12.6 D (TS, shown in the center), and z = 15.1 D (products, shown on the right) for $ClH\cdots OH_2$ in a solvent with $\epsilon_\infty = 2$ and $\epsilon = 13$. In these plots, the abscissa is R_{ClO} in Å and the ordinate is r_{HCl} in Å. The lowest vibrationally adiabatic wave function is shown in the second row from the bottom with the vibrational quantum number increasing up the page. The free-energy surfaces are plotted with the lowest contour representing −24 kcal/mol (−23 kcal/mol for the center panel) and increments of 1 kcal/mol.

to the localized potentials in the r_{HCl} coordinate in the reactant and product regions.

We have assumed an adiabatic separation of time scales between the solvent coordinate motion (orientational polarization) and the vibrations of the solute complex (H atom and H-bond motion). However, we have *not* made any such assumption of separability between these vibrational motions of the solute, e.g., assuming H moves rapidly compared to the Cl−O vibration. Inspection of Figure 2a indicates that the vibrational levels can be assigned except right in the region of the avoided crossings and that the avoided crossings are fairly narrow. This suggests that the Cl−O and Cl−H vibrations are not strongly coupled. Thus, we would expect that the PT would occur adiabatically in the ground and first-excited adiabatic vibrational states. However, in the higher excited vibrational states the dynamics would occur more nonadiabatically (i.e., following the vibrationally diabatic surfaces in Figure 2); this is currently under investigation via examination of the nonadiabatic transition dynamics.[38] For excitation in the proton coordinate (Figure 2b), the latter implication is particularly encouraging for the prospect of infrared-induced PT.[37]

An interesting implication of the free-energy surfaces in Figure 2 is that the barrier height in the solvent coordinate to proton transfer $Cl{-}H\cdots OH_2 \rightarrow Cl^-\cdots HOH_2^+$ is less than k_BT at 300 K. Thus, these model calculations, insofar as they represent the actual $Cl{-}H\cdots OH_2$ system, indicate that the $H{-}Cl{-}H_2O$ acid−base pair in a low-polarity solvent would readily exchange a proton back and forth simply because of thermal fluctuations of the solvent. It is important to distinguish this situation from the often-invoked case of a proton delocalized by tunneling or over-barrier quantum delocalization of the wave function (see, e.g., ref 39). In the present case, the different thermally allowed solvent configurations lead to a thermal distribution of $[Cl{-}H\cdots OH_2]$ and $Cl^-\cdots HOH_2^+$ complexes; in each of these complexes however, the proton is localized on either the acid or the base. Complexes with intermediate natures

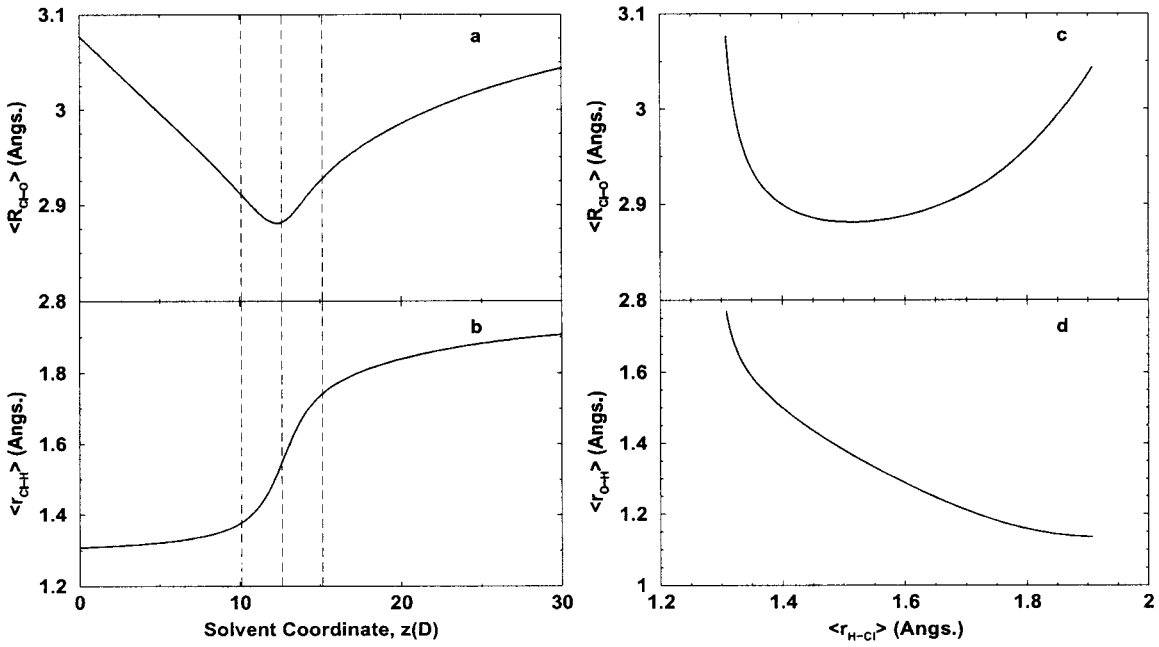

Figure 5. Expectation values of the coordinates (a) R_{ClO} and (b) r_{HCl} as a function of the solvent coordinate z (left panels) for $ClH\cdots OH_2$ in a solvent with $\epsilon_\infty = 2$ and $\epsilon = 13$. Also plotted are (c) $\langle R_{ClO}\rangle$ vs $\langle r_{HCl}\rangle$ and (d) $\langle r_{OH}\rangle$ vs $\langle r_{HCl}\rangle$. In a and b, the vertical dashed lines indicate, from left to right, the value of the solvent coordinate corresponding to the reactants, the TS, and the products for the complex.

(i.e., TS-like) will occur as well, though with slightly less probability, some of which will have a delocalized proton (though not necessarily by tunneling) as illustrated in Figure 3. A similar situation has previously been observed in theoretical studies on a symmetric model PT system with a fixed H-bond coordinate by Borgis et al.[22]

Experimental studies have also found similar hydrogen-bonded complexes.[40,41] Limbach and co-workers have studied a variety of hydrogen-bonded complexes by nuclear magnetic resonance experiments in which the temperature (and hence the solvent dielectric constant) is varied.[40] They find a similar hydrogen-bonding arrangement to that described here in the chloroacetic acid−pyridine complex in mixtures of $CDClF_2$ and CDF_3. That is, their observations are consistent with a "broad distribution of complexes with different structures $A-H\cdots B \rightleftharpoons A^{\delta-}\cdots H\cdots B^{\delta+} \rightleftharpoons A^-\cdots H-B^+$," [40]precisely the situation found here.[42]

B. Coordinate Expectation Values and Variances. One of the advantages of quantizing the two vibrations of the solute together is that we can examine the quantum expectation values of the different coordinates along the reaction coordinate

$$\langle q\rangle(z) = \int \mathrm{d}r_{HCl} \int \mathrm{d}R_{ClO}\, \Psi^*(r_{HCl}, R_{ClO}; z)\hat{q}\Psi(r_{HCl}, R_{ClO}; z) \tag{18}$$

where, e.g., $q = r_{HCl}$ or R_{ClO}. All of the expectation values and variances shown here are for the adiabatic vibrational ground state. The quantum expectation values of r_{HCl} and R_{ClO} as a function of the solvent coordinate are shown in Figure 5 for the $ClH\cdots OH_2$ complex (corresponding to the free-energy surfaces in Figure 2). In Figure 5a, we can see that as the solvent coordinate is increased the average value of R_{ClO} decreases until it reaches a minimum in the region of the TS. In the reactants, $z = z_R$ ($\langle R_{ClO}\rangle = 2.91$ Å), whereas at the TS, $z = z^\ddagger$ ($\langle R_{ClO}\rangle = 2.88$ Å), and in the products, $z = z_P$ ($\langle R_{ClO}\rangle = 2.93$ Å). The reduction in $\langle R_{ClO}\rangle$ leads to a lowering of the barrier for PT (see Figure 2), and the proton is transferred at these smaller H-bond distances. Upon a further increase in the solvent coordinate, past the TS, $\langle R_{ClO}\rangle$ increases as it approaches its equilibrium value in the product $Cl^-\cdots H\cdots OH_2^+$ complex ($z = z_P$, $\langle R_{ClO}\rangle = 2.93$ Å). Note that the average $\langle R_{ClO}\rangle$ distance in the product complex is actually slightly larger than in the reactant complex. This appears to be a reflection of the fact that the solvent prefers the ions in the products separated.

Now turning to Figure 5b, we see that as the solvent coordinate is increased $\langle r_{HCl}\rangle$ increases from 1.38 Å in the reactants to 1.54 Å at the TS region (where the $\langle R_{ClO}\rangle$ distance is shortest) and to 1.74 Å in the products. The changes in $\langle r_{HCl}\rangle$ are clearly correlated with the contraction of the hydrogen-bonded complex (shortening of $\langle R_{ClO}\rangle$) from the reactants to the TS and the subsequent expansion of the complex from the TS to the products. This connection between the movement of the proton and the H-bond coordinate is also seen in the proton potentials shown in Figure 3. It is also illustrated in Figure 5c, where the $\langle R_{ClO}\rangle$ distance is plotted versus $\langle r_{HCl}\rangle$ as the solvent coordinate is varied. Clearly, the location of the proton depends strongly on $\langle R_{ClO}\rangle$. This is evident in the large change in $\langle r_{HCl}\rangle$ when small values of $\langle R_{ClO}\rangle$ are reached.

Another quantity of interest is the variance in the coordinate values:

$$\Delta q(z) = \sqrt{\langle (q - \langle q\rangle)^2\rangle} = [\int \mathrm{d}r_{HCl} \int \mathrm{d}R_{ClO}\, [\Psi^*(r_{HCl}, R_{ClO}; z)](\hat{q} - \langle q\rangle)^2\Psi(r_{HCl}, R_{ClO}; z)]^{1/2} \tag{19}$$

This gives a measure of the localization or delocalization of the vibrational wave function. The values of ΔR_{ClO} and Δr_{HCl} are shown in Figure 6 for the $ClH\cdots OH_2$ complex. From Figure 6a, we can see that as the Cl−O distance is reduced in approaching the TS the wave function becomes more localized in the R_{ClO} coordinate (ΔR_{ClO} decreases), indicating that the well in ΔR_{ClO} is becoming "tighter." The R_{ClO} variance reaches a minimum in the TS region and then increases to its equilibrium value in the product complex as the solvent coordinate is increased. Note that ΔR_{ClO} is smaller in the product complex than in the reactant complex as the zwitterionic character makes the complex more rigid even while $\langle R_{ClO}\rangle$ is slightly larger in the product complex.

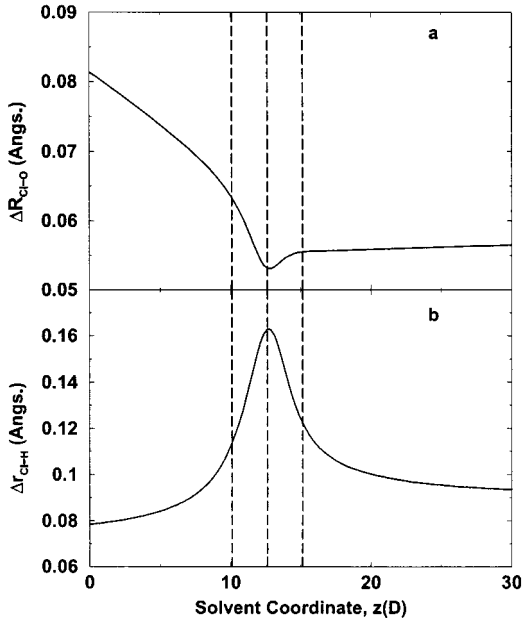

Figure 6. Quantum-mechanical variances in the values of the coordinates (a) R_{ClO} and (b) r_{HCl} as a function of the solvent coordinate z for $ClH\cdots OH_2$ in a solvent with $\epsilon_\infty = 2$ and $\epsilon = 13$. The vertical dashed lines indicate, from left to right, the value of the solvent coordinate corresponding to the reactants, the TS, and the products.

In the variance in the r_{HCl} coordinate, shown in Figure 6b, we can observe the passage of the complexes from localized (as $ClH\cdots OH_2$) to delocalized (at the TS) where the PT occurs to localized again (as $Cl^-\cdots HOH_2^+$) as the solvent coordinate is increased. This behavior can also be seen in Figues 2 and 3 on the basis of the nature of the potential felt by the proton in the reactants, TS, and products along with the position of the levels.

From the combination of all of these results, we can infer how the PT reaction proceeds through solvent coordinate changes. With the solvent coordinate in equilibrium with the reactant complex, the proton potential has a global minimum at small r_{HCl} values and the proton, in its vibrational ground state, is localized on the acid. As the solvent coordinate increases, the acid−base complex contracts, reducing the Cl−O distance and leading to a nearly symmetric double-well proton potential (see Figure 3). The proton is then quantum-mechanically delocalized between the acid and the base in its vibrational ground state; this represents the TS for the PT in the solvent coordinate. Increasing the solvent coordinate further leads to a expansion of the complex (R_{ClO} increases) and a global minimum in the proton potential at larger r_{HCl} distances. Thus, the products are reached, and the proton is localized on the base.

IV. Concluding Remarks

We have developed a model description for the acid−base PT reaction between HCl and H_2O in a hydrogen-bonded complex dissolved in a low-polarity solvent. In this description, a two VB state perspective consistent with the Mulliken picture of PT is employed and the nonequilibrium polarization of the solvent is characterized via the Kim−Hynes theoretical approach.

The reaction free-energy surface for the resulting nearly thermodynamically symmetric reaction was analyzed, with special attention to the quantum nuclear aspects of the proton and H-bond coordinate vibrations. In particular, the vibrational wave functions in these two coordinates were followed along the solvent coordinate reaction path, and the vibrational states of the reacting system were discussed. For the latter, analysis indicates that the PT reaction in the ground and lowest excited levels is vibrationally adiabatic; however, for higher levels involving excitation in the proton coordinate, a different view is suggested, an issue of relevance for the possibilities of infrared-induced PT in solution.

The calculated low free-energy barrier for the model reaction indicates a facile thermal interconversion between the molecular pair reactant and contact ion pair product within the complex. We are unaware of any experimental studies examining complexes of HCl (or other hydrogen halides) and H_2O in low-polarity solvents. However, it has been established for some time that acid−base pairs dissolved in low-polarity solvents exist as hydrogen-bonded complexes (i.e., the complex does not dissociate) in either the $A-H\cdots B$ or the $A^-\cdots H-B^+$ form, depending on the relative strength of the acid and base.[43] It would clearly be of interest if the ready thermal interconversion between reactants and products observed here could be directly observed experimentally.

Finally, the basic approach employed within could be used to examine the trends of the activation free-energy barriers for the hydrogen halide acids complexed with water in low-polarity solvents. It is considered well established that the thermodynamic acidity of the hydrogen halide acids increases down the periodic table column (from F to I). Although there are many factors that determine the acidity of these acids, this trend has generally been attributed to the decreasing homolytic BDE in the series.[44] However, how the BDE affects the free-energy barrier height in acid−base PT reactions is significantly less clear (though at least one simple model[45] has been proposed to predict the behavior in the special case of certain radical cation acids). This aspect, together with the related issue of the relationship between the free-energy barrier and the reaction free energy,[36,45−47] is left for future research.

Acknowledgment. This paper is dedicated to Prof. William H. Miller on the occasion of his 60th birthday. W.H.T. is indebted to Bill for his guidance, support, and encouragement. This work was supported in part by NSF Grant CHE-9700419. We thank Dr. Phillip M. Kiefer for many useful discussions.

Appendix: Dependence of the Electronic Coupling on the Proton Coordinate

In this Appendix, we consider the dependence of the electronic coupling on the proton coordinate. Previously, Timoneda and Hynes[20] (TH) argued that, in the case of a phenol−amine PT, the coupling should be effectively independent of the proton coordinate. Here we reprise that argument and show that the result is different in the present case of hydrochloric acid and water.

In their study, TH used a VB description that differs only slightly from that used here (a polarization component $[A^-H^+-B]$ was added to the covalent state with a fixed contribution). They evaluated the overlap of the covalent and ionic VB states that is naturally related to the electronic coupling. Their result, applied to the present system, is that

$$\langle\phi_c|\phi_c\rangle = \left[\frac{2}{1-\langle H|B\rangle^2+\langle H|A\rangle^2}\right]^{1/2}\left[\frac{2}{1-\langle H|A\rangle^2+\langle H|B\rangle^2}\right]^{1/2}\langle H|A\rangle\langle H|B\rangle \quad (20)$$

where $|A\rangle$ represents the valence orbital on the acid and $|B\rangle$ the valence orbital on the base. This expression is derived by ignoring the overlap $\langle A|B\rangle$, which is a good approximation. In

the phenol-amine case, considered by TH, $|A\rangle$ is a 2p orbital on the oxygen atom of the phenol, $|B\rangle$ is a 2p orbital on the nitrogen atom of the amine, and $|H\rangle$ is the 1s orbital on the hydrogen. Using interpolation formulas for calculating the overlap between Slater orbitals,[48] they found that as the proton is moved between A and B that, e.g., the $\langle H|A\rangle$ overlap decreases and the $\langle H|B\rangle$ increases in such a way that their product is roughly constant.

In the present case, $|A\rangle$ is the 3p orbital on the chlorine atom and $|B\rangle$ is the 2p orbital on the oxygen atom of water. The same analysis for this situation yields the result that $\langle H|A\rangle$ and $\langle H|B\rangle$ do not increase and decrease commensurately, and thus the overlap $\langle\phi_c|\phi_i\rangle$ is not constant with respect to the proton coordinate. This is an initial indication that for this system the electronic coupling should not be expected to be constant with respect to the H coordinate and is consistent with the results obtained from our two-state VB model, as is indicated in Figure 1.

References and Notes

(1) Ando, K.; Hynes, J. T. *J. Phys. Chem. B* **1997**, *101*, 10464−10478. Ando, K.; Hynes, J. T. *J. Mol. Liq.* **1995**, *64*, 25−37.

(2) (a) Gertner, B. J.; Hynes, J. T. *Science* **1996**, *271*, 1563. (b) Gertner, B. J.; Hynes, J. T. *Faraday Discuss.* **1998**, *110*, 301.

(3) Hanson, D. R.; Ravishankara, A. R. *J. Phys. Chem.* **1992**, *96*, 2682−2691. Molina, M. J. *The Chemistry of the Atmosphere: Its Impact on Global Change*; IUPAC, Blackwell: Oxford, U.K., 1994; p 27. Thibert, E.; Dominé F. *J. Phys. Chem. B* **1997**, *101*, 3554. Graham, J. D.; Roberts, J. T. *J. Phys. Chem.* **1994**, *98*, 5764.

(4) Morris, J. R.; Behr, P.; Antman, M. D.; Ringeisen, B. R.; Splan, J.; Nathanson, G. M. *J. Phys. Chem. A* **2000**, *104*, 6738−6751.

(5) Clary, D. C.; Wang, L. C. *J. Chem. Soc., Faraday Trans.* **1997**, *93*, 2763−2767. Robertson, S. H.; Clary, D. C. *Faraday Discuss.* **1995**, *100*, 309−320. Estrin, D. A.; Kohanoff, J.; Laria, D. H.; Weht, R. O.; *Chem. Phys. Lett.* **1997**, *280*, 280−286. Allouche, A.; Couteurier-Tamburelli, I.; Chiavassa, T. *J. Phys. Chem. B* **2000**, *104*, 1497−1506.

(6) Kroes, G. J. *Comments At. Mol. Phys.* **1999**, *34*, 259.

(7) Laasonen, K. E.; Klein, M. L. *J. Phys. Chem. A* **1997**, *101*, 98. Laasonen, K. E.; Klein M. L. *J. Am. Chem. Soc.* **1994**, *116*, 11620. Balbuena, P. B.; Johnston, K. P.; Rossky, P. J. *J. Phys. Chem.* **1996**, *100*, 2716.

(8) Marx, D.; Tuckerman, M. E.; Hutter, J.; Parrinello, M. *Nature* **1999**, *397*, 601.

(9) Hynes, J. T. *Nature* **1999**, *397*, 565.

(10) Schmitt, U. W.; Voth, G. A. *J. Chem. Phys.* **1999**, *111*, 9361−9381. Schmitt, U. W.; Voth, G. A. *Isr. J. Chem.* **1999**, *39*, 483−492.

(11) Hammes-Schiffer, S.; Tully, J. C. *J. Chem. Phys.* **1994**, *101*, 4567−4667. Hammes-Schiffer, S.; Tully, J. C. *J. Phys. Chem.* **1995**, *99*, 5793−5797.

(12) Hammes-Schiffer, S. *J. Phys. Chem. A* **1998**, *102*, 10443−10454.

(13) Staib, A.; Borgis, D.; Hynes, J. T. *J. Chem. Phys.* **1995**, *102*, 2487−2505.

(14) Borgis, D.; Hynes, J. T. *J. Phys. Chem.* **1996**, *100*, 1118−1128; Borgis, D.; Hynes, J. T. *Chem. Phys.* **1993**, *170*, 315−346. Borgis, D.; Hynes, J. T. *J. Chem. Phys.* **1991**, *94*, 3619−3628. Borgis, D.; Lee, S.-Y.; Hynes, J. T. *Chem. Phys. Lett.* **1989**, *162*, 19−26.

(15) Vuilleumier, R.; Borgis, D. *J. Chem. Phys.* **1999**, *111*, 4251−4266. Vuilleumier, R.; Borgis, D. *J. Phys. Chem. B* **1998**, *102*, 4261−4264. Azzouz, H.; Borgis, D. *J. Mol. Liq.* **1995**, *63*, 89−107.

(16) Ando, K.; Hynes, J. T. *Discuss. Faraday Soc.* **1995**, *102*, 435−441. Ando, K.; Hynes, J. T. *J. Phys. Chem. A* **1999**, *103*, 10398−10408.

(17) Ando, K.; Hynes, J. T. *Adv. Chem. Phys.* **1999**, *110*, 381−430 and references therein.

(18) Mulliken, R. S. *J. Phys. Chem.* **1952**, *56*, 801−822. Mulliken, R. S. *J. Chim. Phys. Phys.-Chim. Biol.* **1964**, *61*, 20−36. Mulliken, R. S.; Person, W. B. *Molecular Complexes*; Wiley-Interscience: New York, 1969.

(19) Bratož, S. *Adv. Quantum Chem.* **1967**, *3*, 209−237. Ratajczak, H. *J. Phys. Chem.* **1972**, *76*, 3000−3004; 3991−3992. Zwilles, B. A.; Person, W. B. *J. Chem. Phys.* **1983**, *79*, 65.

(20) Timoneda, J.; Hynes, J. T. *J. Phys. Chem.* **1991**, *95*, 10431−10442.

(21) See also, Thompson, W. H.; Hynes, J. T. *J. Am. Chem. Soc.* **2000**, *122*, 6278−6286.

(22) Borgis, D.; Tarjus, G.; Azzouz, H. *J. Phys. Chem.* **1992**, *96*, 3188−3191. Borgis, D.; Tarjus, G.; Azzouz, H. *J. Chem. Phys.* **1992**, *97*, 390−400.

(23) Warshel, A. *J. Phys. Chem.* **1982**, *86*, 2218; Warshel, A. *Computer Modeling of Chemical Reactions in Enzymes and Solutions*; Wiley: New York, 1991.

(24) It is clear that the bend coordinate of the hydrogen bond complex may play an important role in the energetics and dynamics of the PT reaction. However, for simplicity, this coordinate is frozen in the present study, and this aspect of the problem will be addressed in future work.

(25) All ab initio calculations reported in this paper were carried out using Frisch, M. J.; Trucks, G. W.; Schlegel, H. B.; Scuseria, G. E.; Robb, M. A.; Cheeseman, J. R.; Zakrzewski, V. G.; Montgomery, J. A., Jr.; Stratmann, R. E.; Burant, J. C.; Dapprich, S.; Millam, J. M.; Daniels, A. D.; Kudin, K. N.; Strain, M. C.; Farkas, O.; Tomasi, J.; Barone, V.; Cossi, M.; Cammi, R.; Mennucci, B.; Pomelli, C.; Adamo, C.; Clifford, S.; Ochterski, J.; Petersson, G. A.; Ayala, P. Y.; Cui, Q.; Morokuma, K.; Malick, D. K.; Rabuck, A. D.; Raghavachari, K.; Foresman, J. B.; Cioslowski, J.; Ortiz, J. V.; Stefanov, B. B.; Liu, G.; Liashenko, A.; Piskorz, P.; Komaromi, I.; Gomperts, R.; Martin, R. L.; Fox, D. J.; Keith, T.; Al-Laham, M. A.; Peng, C. Y.; Nanayakkara, A.; Gonzalez, C.; Challacombe, M.; Gill, P. M. W.; Johnson, B. G.; Chen, W.; Wong, M. W.; Andres, J. L.; Head-Gordon, M.; Replogle, E. S.; Pople, J. A. *Gaussian 98*, revision A.6; Gaussian, Inc.: Pittsburgh, PA, 1998.

(26) The optimized geometry calculated by MP2/6-31++G** calculations gives $r_{HCl} = 1.28$ Å, $r_{OH} = 1.90$ Å, $R_{ClO} = 3.19$ Å, and $r_{OHw} = 0.964$ Å. The H−O−H angle in the water molecule is 106.0°, and the Cl−H−O angle is 178.5°.

(27) Re, S.; Osamura, Y.; Suzuki, Y.; Schaefer, H. F., III. *J. Chem. Phys.* **1998**, *109*, 973−977.

(28) Szczeñniak, M. M.; Scheiner, S.; Bouteiller, Y. *J. Chem. Phys.* **1984**, *81*, 5024−5030.

(29) The Morse potential at small r typically is not as strongly repulsive as that found, for example, in ab initio calculations.

(30) Roszak, S. *Chem. Phys. Lett.* **1996**, *250*, 187−191.

(31) Press, W. H.; Flannery, B. P.; Teukolsky, S. A.; Vetterling, W. T. *Numerical Recipes, The Art of Scientific Computing*; Cambridge University Press: Cambridge, U.K., 1992.

(32) Kim, H. J.; Hynes, J. T. *J. Chem. Phys.* **1992**, *96*, 5088.

(33) Grasselli, J. G., Ritchey, W. M., Eds.; *Atlas of Spectral Data and Physical Constants for Organic Compounds*; The Chemical Rubber Company: Cleveland, OH, 1975.

(34) One could equivalently use an energy gap coordinate (see, e.g., ref 17) to characterize a solvent coordinate. For the present purposes, the coordinate z is slightly preferable in that it gives a sense of the polarization state in the solvent via eq 12.

(35) Colbert, D. T.; Miller, W. H. *J. Chem. Phys.* **1992**, *96*, 1982−1991.

(36) Kiefer, P. M.; Hynes, J. T. *Nonlinear Free Energy Relationships for Adiabatic Proton-Transfer Reactions in a Polar Environment; I. Fixed Proton Donor−Acceptor Distance* and *Nonlinear Free Energy Relationships for Adiabatic Proton-Transfer Reactions in a Polar Environment. II. Inclusion of Proton Donor−Acceptor Vibration*; Manuscripts in preparation.

(37) Kim, H. J.; Staib, A.; Hynes, J. T. In *Ultrafast Reaction Dynamics at Atomic-Scale Resolution Femtochemistry and Femtobiology, Nobel Symposium 101*; Sundstrom, V., Ed.; Imperial College Press: London, 1998.

(38) Laage, D.; Thompson, W. H.; Hynes, J. T. Work in progress.

(39) Cleland, W. W.; Kreevoy, M. M. *Science* **1994**, *267*, 1887.

(40) Golubev, N. S.; Denisov, G. S.; Smirnov, S. N.; Shchepkin, D. N.; Limbach, H.-H. *Z. Phys. Chem.* **1996**, *196*, 73−84.

(41) Perrin, C. L.; Nielsen, J. B. *Annu. Rev. Phys. Chem.* **1997**, *48*, 511−544.

(42) On a related point, Golubev et al.[40] have examined the HCl and pyridine acid−base pair and find that under the conditions of their experiment it only exists in the ionized form of chloride ion and pyridinium. This is not inconsistent with the present results involving water, a much weaker base.

(43) King, E. J. In *Physical Chemistry of Organic Solvent Systems*; Covington, A. K., Dickinson, T., Eds.; Plenum Press: New York, 1973; pp 331−388.

(44) See, for example, Zumdahl, S. S.; Zumdahl, S. A. *Chemistry*; Houghton Mifflin: New York, 2000.

(45) Anne, A.; Hapiot, P.; Moiroux, J.; Neta, P.; Savéant, J.-M. *J. Am. Chem. Soc.* **1992**, *114*, 4694−4701. Anne, A.; Fraoua, S.; Grass, V.; Moiroux, J.; Savéant, J.-M. *J. Am. Chem. Soc.* **1998**, *120*, 2951−2958.

(46) Marcus, R. A. *Faraday Symp. Chem. Soc.* **1975**, *10*, 60. Marcus, R. A. *J. Phys. Chem.* **1968**, *72*, 891. Cohen, A. O.; Marcus, R. A. *J. Phys. Chem.* **1968**, *72*, 4249. Marcus, R. A. *J. Am. Chem. Soc.* **1969**, *91*, 7224. Agmon, N. *Int. J. Chem. Kinet.* **1981**, *13*, 333.

(47) Pines, E.; Magnes, B.-Z.; Lang, M. J.; Fleming, G. R. *Chem. Phys. Lett.* **1997**, *281*, 413. Kreevoy, M. M.; Konasewich, D. E. *Adv. Chem. Phys.* **1972**, *21*, 243. Kreevoy, M. M.; Oh, S.-W. *J. Am. Chem. Soc.* **1973**, *95*, 4805. Kresge, A. J. *Acc. Chem. Res.* **1975**, *8*, 354. Kresge, A. J.; Silverman, D. N. *Methods Enzymol.* **1999**, *308*, 276.

(48) Mulliken, R. S.; Rieke, C. A.; Orloff, D.; Orloff, H. *J. Chem. Phys.* **1949**, *17*, 1248.